PROBE-FED RECTANGULAR DIELECTRIC RESONATOR ANTENNAS: THEORETICAL MODELLING & EXPERIMENTS

M. H. Neshati[1] and Z. Wu[2]

1: Electrical Dept., Sistan & Baluchistan Univ. Zahedan, 98164, Iran.
e-mail: neshat@hamoon.usb.ac.ir

2: Electrical & Electronics Engineering Dept., UMIST,
Manchester M60 1QD, UK.
e-mail: z.wu@umist.ac.uk

Keywords: Dielectric Resonator Antenna, Conventional Dielectric Waveguide Model and Finite Element Method

ABSTRACT: A Rectangular Dielectric Resonator Antenna (RDRA) is theoretically analysed using the Conventional Dielectric Waveguide Model (CDWM), numerically simulated using the High Frequency Structure Simulator (HFSS) based on the Finite Element Method (FEM) software package and experimentally investigated with the consideration of the fundamental mode TE_{111}. Antenna parameters under investigation include resonance frequency, radiation patterns, directivity, Q-factor, impedance bandwidth and cross polarisation level. The results for a specific resonator are presented and compared with those obtained by experiments. It is concluded that the CDWM can be used for a first order estimation of the antenna parameters, but more accurate results can be obtained using the FEM for radiation patterns.

1. INTRODUCTION

Dielectric Resonators (DRs) made of low loss and high dielectric constant ceramic materials have been extensively studied in the past decades for designing miniaturised shielded microwave circuits and have been well used in filters and oscillators as a tuning element. With an appropriate feed arrangement, they can also be used as antennas and they provide efficient radiation due to non-metallic loss that may prove beneficial in the microwave and millimetre region [1-12]. The other advantages of the Dielectric Resonator Antennas (DRAs) are small size, low cost, large bandwidth and simple coupling structures in compare to the conventional antennas. The most common shapes of the DRs are cylindrical [1, 4, 6,], rectangular [2, 6, 8, 9, 12] and hemispherical [3]. Compared with the other geometry's, Rectangular Dielectric Resonators (RDRs) are more attractive for their easier fabrication and also the existence of two independent aspect ratios for a better design flexibility to obtain impedance matching and radiation requirements. More significantly, in rectangular DRs, mode degeneracy [6] can be avoided by properly choosing the dimensions and hence lower cross polarisation is obtained.

In this paper a probe-fed rectangular DRA, positioned on top of a ground plane, is studied theoretically and experimentally. Two different modelling techniques, namely the Conventional Dielectric Waveguide Model (CDWM) and the Finite Element Method (FEM) are utilised to estimate the radiation parameters of the RDRA.

2. THE ANTENNA STRUCTURE

Figure 1 shows the RDRA structure under investigation. The resonator dimensions are a, b and h along x-, y- and z-direction respectively and its relative dielectric constant is ε_r. A circular metallic plate with a diameter d is the ground

plane and supports the resonator. A vertically oriented small coaxial probe through an SMA connector excites the resonator at the dominant mode TE^{y}_{111} [6]. The probe is located at x=a/2 and φ=0° and its height is equal to that of the DR.

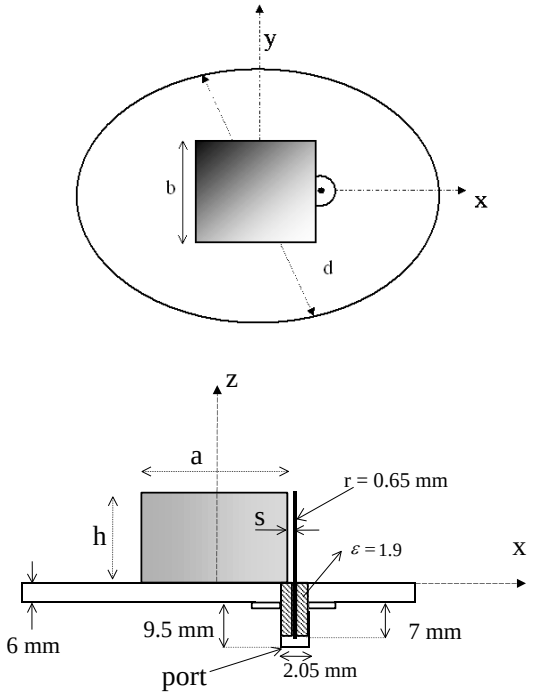

Figure 1: The structure of the RDRA under consideration: a) Top View b) Side view

3. THE CONVENTIONAL DIELECTRIC WAVEGUIDE MODEL (CDWM)

For the theoretical formulation, the effect of the probe is neglected and as an approximation, the ground plane is considered to be infinitely large. Image theory is then applied to replace the ground with an image resonator extending to z =-h. The equivalent isolated resonator is fed by a dipole of twice the length of the probe. Based on the CDWM theory, the isolated resonator is assumed to be the truncation of an infinite rectangular dielectric waveguide. Hence, the modes of the operation are similar to those of a long dielectric waveguide. The field components of the fundamental mode inside the resonator are obtained by solving Maxwell's equations with perfect magnetic wall (PMW) boundary conditions at x= ±a/2and z= ±h and continuous tangential fields at y= ±b/2 [6]. They are given as:

$$E_x = -(A/\varepsilon_d)k_z \cos(k_x x)\cos(k_y y)\sin(k_z z)$$

$$E_y = 0$$

$$E_z = (A/\varepsilon_d)k_x \sin(k_x x)\cos(k_y y)\cos(k_z z)$$

$$H_x = (A/j\omega\mu_0\varepsilon_d)(k_x k_y)\sin(k_x x)\sin(k_y y)\cos(k_z z)$$

$$H_y = (A/j\omega\mu_0\varepsilon_d)(k_x^2 + k_z^2)\cos(k_x x)\cos(k_y y)\cos(k_z z)$$

$$H_z = (A/j\omega\mu_0\varepsilon_d)(k_y k_z)\cos(k_x x)\sin(k_y y)\sin(k_z z)$$

where $\varepsilon_d=\varepsilon_0\cdot\varepsilon_r$. The characteristic equations for the TE^{y}_{111} mode are:

$$\begin{aligned} &k_x = (\pi/a), \\ &k_y \tan(k_y b/2) = \sqrt{k_x^2 + k_z^2 - k_0^2}, \\ &k_z = (\pi/2h) \end{aligned} \qquad (1)$$

and the resonance frequency is the solution of the separation equation given by:

$$\varepsilon_r k_0^2 = k_x^2 + k_y^2 + k_z^2 \qquad (2)$$

where $k_0 = \omega/c$ is the free space wave number.

The radiation fields of the RDRA are due to the equivalent magnetic currents $\mathbf{M}(x', y', z')$ on the surfaces of the resonator given by [13]:

$$\mathbf{M} = \mathbf{E} \times \hat{n}$$

where $\hat{n}$ is a unit vector normal to the surface pointing out and E is the electric field on the surface of the resonator. The electric vector potential produced by the magnetic currents is given by [13]:

$$\mathbf{F} = \frac{\varepsilon_0}{4\pi} \iint_S \frac{\mathbf{M}}{R} e^{-jkR} ds' \qquad (3)$$

where R is the distance between the source point and the observation point.

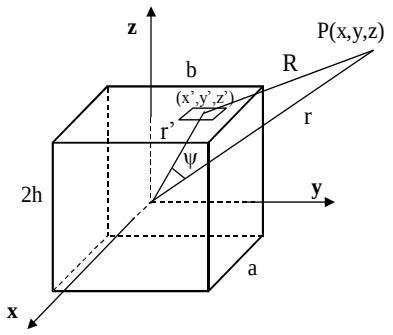

Figure 2: The equivalent model of the ground-backed RDRA and the observation point for the far field calculation.

In the far field region, the distance R from any point on the surface of the resonator to the observation point P can be assumed to be parallel to the radial vector distance **r** from the origin (centre of the resonator) to the point P. In this

case, the electric vector potential can be simplified to:

$$\mathbf{F} \approx \frac{\varepsilon_0 \, e^{-jk_0 r}}{4\pi r}\mathbf{L} \tag{4}$$

where

$$\begin{aligned}\mathbf{L} &= \iint_S \mathbf{M} e^{-jk_0 r' \cos\psi} ds' = \\ &\iint_S (M_x \hat{a}_x + M_y \hat{a}_y + M_z \hat{a}_z) ds'\end{aligned} \tag{5}$$

In the far field region only θ and ϕ field components are important, as the radial field component is significantly small in comparison with other components [14]. The field components in the far field region are given by:

$$\begin{aligned} E_\theta &\approx -\frac{jk_0 e^{-jkr}}{4\pi r} L_\phi, \quad E_\phi \approx +\frac{jk_0 e^{-jkr}}{4\pi r} L_\theta \\ H_\theta &= +\frac{E_\theta}{\eta_0}, \quad H_\phi = -\frac{E_\phi}{\eta_0} \end{aligned} \tag{6}$$

It can be shown that

$$L_\phi = \left(\frac{2A\pi^2}{\varepsilon_d ah}\right) \cdot \cos\phi \cos(k_0 \frac{a}{2} \sin\theta \cos\phi) \cos(k_0 h \cos\theta) \left\{\frac{D_1}{D_2} + \frac{2D_1}{D_3}\right\}$$
$$+ \left(\frac{2Ak_0 k_x \pi}{\varepsilon_d h}\right) \cdot \cos(\delta\pi/2) \cdot \sin\theta \sin(2\phi) \sin(k_0 \frac{b}{2} \sin\theta \sin\phi) \cdot$$
$$\cos(k_0 h \cos\theta) \cdot \cos(k_0 \frac{a}{2} \sin\theta \cos\phi) \cdot \frac{1}{D_2 \cdot D_3}$$

and

$$L_\theta = \left(\frac{2A\pi^2}{\varepsilon_d ah}\right) \cos\theta \sin\phi \cos(k_0 \frac{a}{2} \sin\theta \cos\phi) \cdot$$
$$\cos(k_0 h \cos\theta) \frac{D_1}{D_2} + \left(\frac{2A\pi k_0 k_x}{\varepsilon_d h}\right) \cos(\delta\pi/2) \sin 2\theta \cos^2\phi \cdot$$
$$\sin(k_0 \frac{b}{2} \sin\theta \sin\phi) \cdot \cos(k_0 h \cos\theta) \cos(k_0 \frac{a}{2} \sin\theta \cos\phi) \frac{1}{D_2 \cdot D_3}$$

with

$$D_1 = \left(\frac{\sin(k_0 \frac{b}{2} \sin\theta \sin\phi + \delta\pi/2)}{k_0 \sin\theta \sin\phi + \delta\pi/b} + \frac{\sin(k_0 \frac{b}{2} \sin\theta \sin\phi - \delta\pi/2)}{k_0 \sin\theta \sin\phi - \delta\pi/b} \right)$$

$$D_2 = (\pi/2h)^2 - (k_0 \cos\theta)^2, \; D_3 = (\pi/a)^2 - (k_0 \sin\theta \cos\phi)^2$$

The directivity of the RDRA can be calculated using the equation given by [14] :

$$D_{max} = \frac{(E_\theta^2(\theta,\phi) + E_\phi^2(\theta,\phi))_{max}}{\frac{1}{4\pi} \int_0^{2\pi} \int_0^{\pi} (E_\theta^2(\theta,\phi) + E_\phi^2(\theta,\phi)) \sin\theta d\theta d\phi} \tag{7}$$

The Q-factor of the RDRA is defined as

$$Q_0 \approx Q_r = \omega W / P_r$$

where W is the stored energy inside the resonator and P_r is the total radiated power by the RDRA, which are given respectively by:

$$\begin{aligned} W &= \frac{A^2}{32\varepsilon_d} abh(1 + \frac{\sin(k_y b)}{k_y b})(k_x^2 + k_z^2) \; , \\ P_r &= \frac{1}{4} \frac{1}{\eta_0} \int_0^{2\pi} \int_0^{2\pi} (|E_\theta|^2 + |E_\phi|^2) r^2 \sin\theta \, d\theta \, d\phi \end{aligned} \tag{8}$$

For Q-factor measurement, the unloaded Q-factor, Q_0, of the RDRA can be obtained using the one port reflection coefficient measurement discussed in [15] and the impedance bandwidth of the RDRA (VSWR ≤ 2.6) is approximately related to the Q_0 factor by:

$$BW(\%) \approx (100/Q_0)$$

4. THE FINITE ELEMENT MODEL

The RDRA in Figure 1 is numerically investigated using the HP85180A High Frequency Structure Simulator (HFSS) [16]. The HFSS is a software package based on the FEM. In general, in the HFSS, the geometric model is divided into a large number of elements, which are thetrahedra, where a single thetraherdon is basically a four-sided pyramid.

The value of a vector quantity such as **E**- or **H**-field inside each element is obtained by interpolation from the vertices of the tetrahedron. The antenna structure is surrounded by an absorbing surface with the second order radiation boundary condition given by [12]:

$$\begin{aligned}(\nabla \times \mathbf{E})_{tan} &= jk_0 (\mathbf{E})_{tan} - (j/k_0) \nabla_{tan} \times (\nabla_{tan} \times \mathbf{E}_{tan}) \\ &+ (j/k_0) \nabla_{tan} (\nabla_{tan} \cdot \mathbf{E}_{tan})\end{aligned} \tag{9}$$

where $\mathbf{E}_{\tan}$ is the tangential component of the **E**-field on the surface. The absorbing surface represents as an open space and is allowed to radiate the waves instead of being contained within it. This radiation surface does not have to be spherical. The only restriction regarding to the shape is that it has to be convex with regard to the source and to ensure accurate results, it should be placed at least a quarter of wavelength away from the radiation source.

The HFSS then maps the **E**-field computed in (4) on the absorbing surface and calculates the far-field and radiation patterns using

$$\mathbf{E}(x,y,z) = \int_s \left[\begin{array}{l} (j\omega\mu_0 \mathrm{H}_{tan}) G + (\mathbf{E}_{tan} \times \nabla G) \\ + (\mathbf{E}_{normal} \times \nabla G) \end{array} \right] ds \tag{10}$$

where $\mathbf{E}_{\tan}, \mathbf{H}_{\tan}$ are the tangential components of electric and magnetic fields respectively and $\mathbf{E}_{\text{normal}}$ is the normal component of the electric field on the radiation surface *s*, and *G* is the free space Green's Function.

5. RESULTS

For a specific dielectric resonator with a=19 mm b=19 mm, h=9.5 mm and ε_r=38 supported by a circular ground plane with d= $\propto$ and d=10cm, the results of theoretical and numerical analysis are listed in Table 1, together with the corresponding measured values for d=10 cm. The radiation patterns for d=$\propto$ and d=10 cm are shown in Figures 3 and 4 respectively.

It can be seen that, for d= $\propto$ predicted resonance frequency using the CDWM is less than that of the FEM with only 1.5% difference. The simulated Q-factor, using the HFSS, differed from the CDWM ones by +12% and so, the impedance bandwidth predicted value is lower by the same factor. The predicted radiation patterns using the CDWM and HFSS agree very well. Also the directivity agrees well with an error of 10%.

In case of the finite ground plane, the predicted resonance frequency and Q-factor using the HFSS have an error of -5% and +19% respectively in compare to the measured ones. These errors are due to the existence of thin air gaps between the resonator and ground plane and also between the RDRA and feed probes, which are not included in the simulation. It can be observed that there is only difference in simulated and measured E-Plane radiation patterns compared with the CDWM at small elevation angles near the ground plane. This is believed to be due to the effect of the finite size of the ground. As a result the numerical method produces more accurate radiation patterns. The simulated result for the directivity has not such good agreement compare to the experiment where the error can be high as +28.5%. It is said that this error is because of the non-convergence of the numerical method in the allowed run time of the simulation. However, the CDWM has more accurate result for the directivity. The difference between measured and simulated cross-polarisation level is 12.5 dB.

6. CONCLUSIONS

Two different modelling methods are used for investigating a rectangular DRA. Results indicate that the CDWM predicts a first order estimation of the RDRA radiation parameters and the HFSS can produce more accurate radiation patterns. However, the radiation patterns are affected by the finite size of the ground plane at small angles near to the ground plane. Also there is an error in the simulated resonance frequency and Q-factor in compare to the experimental results in case of finite ground plane. The effects of finite size of ground plane and air gaps in the antenna structures need to be taken into consideration in the theoretical modelling to produce more accurate prediction of radiation parameters, in which case the CDWM has its limitation.

Table 1. Radiation characteristics of the RDRA on a circular ground plane

Parameter	**CDWM** d=$\propto$	**FEM**		**Measured** *d=10cm*
		d=$\propto$	*d=10cm*	
Frequency (GHZ)	2.022	2.053	2.078	2.175
Q-Factor	33.088	37.185	36.793	30.906
Bandwidth (VSWR<2.5) (%)	2.850	2.551	2.578	3.075
Directivity or Gain	2.881	3.198	4.629	3.344
Cross-Polarisation level (dB) at θ=0°	_	_	33.959	21.425

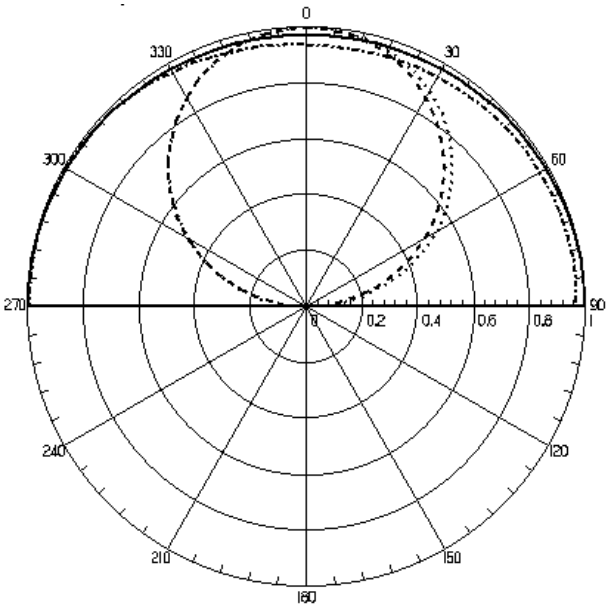

Figure 3: Theoretical co-polarisation radiation patterns of the RDRA on an infinite ground plane.
(CDWM: ——— E_θ at ϕ= 0° - - - - E_ϕ at ϕ=90°)
(FEM: _ . _ . _ E_θ at ϕ= 0°..... E_ϕ at ϕ=90°)

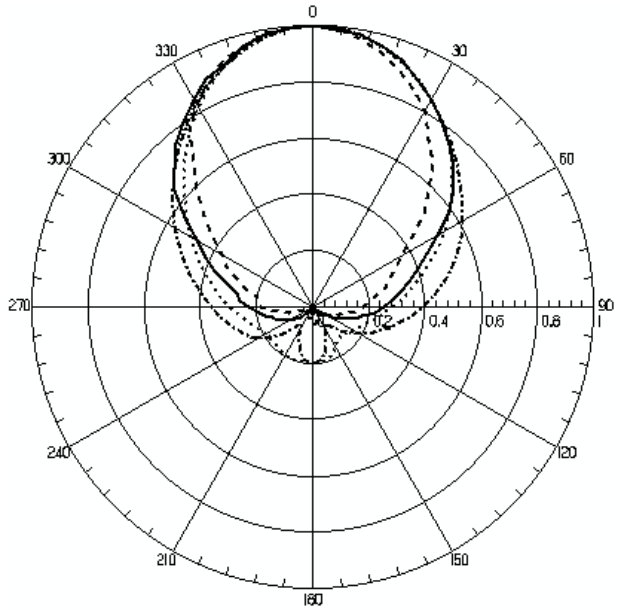

Figure 4: Theoretical and measured co-polarisation radiation patterns of the RDRA on a finite circular ground plane d=10cm.

(Measured: ——— E_θ at ϕ= 0° - - - - E_ϕ at ϕ=90°)
(The FEM: — · — E_θ at ϕ= 0° ..... E_ϕ at ϕ=90°)

REFRENCES

[1] Long S. T., McAllister M. W. and Shen L. C., "The Resonant Cylindrical Dielectric Cavity Antenna", IEEE Transactions on Antenna & Propagation, Vol. AP-33, 1983, pp. 406-412.

[2] M. W. McAllister, S. A. Long And G. L. Conway, "Rectangular Dielectric Resonator Antenna", Electronics Letters, Vol. 19, 1983, pp. 218-219.

[3] M. W. McAllister and S. A. Long, "Resonant Hemispherical Dielectric Antenna", Electronics Letters, vol. 20, pp. 657-659, 1984.

[4] R. K. Mongia, A. Ittipiboon, Y. M. M. Antar, P. Bhariat, and M. Cuhaci, "A Half Spilt Cylindrical Dielecric Resonator Antenna Using Slot Coupling", IEEE Microwave and Guided Waves Letters, vol. 3, pp. 38-39, 1993.

[5] R. K.Mongia, and P. Bhartia "Dielectric Resonator Antenna - A Review and General Design Relations to Resonant Frequency and Bandwidth", International Journal of Microwave and Millimetre-Wave Computer Aided Engineering, Vol. 4,1994, pp. 230-247.

[6] R. K. Mongia, and A. Ittipiboon, "Theoretical and Experimental Investigations on Rectangular Dielectric Resonator Antennas", IEEE Transaction on Antenna and Propagation, Vol. AP-45, 1997, pp. 1348-1356.

[7] G. Drossos, Z. Wu, and L.E. Davis, "Cylindrical Dielectric Resonator Antennas: Theoretical Modelling and Experiments", Microwave & Communication Technologies Conference (M&RF'97), Wembley Conference Centre, London, UK, pp. 34-39.

[8] Neshati M. H. and Wu, Z., "Theoretical and Experimental Investigation of Probe-fed Rectangular Dielectric Resonator Antennas." Millennium Conference on Antennas & Propagation, AP2000, Davos, Switzerland.

[9] Neshati M. H. and Wu, Z., "Rectangular Dielectric Resonator Antennas: Theoretical Modelling and

Experiments.", 11th International Conference on Antenna and Propagation (ICAP2001), 17-20 April 2001, UMIST, Manchester, UK, Vol. 480, pp. 886-870.

[10] Petosa, A. Ittipiboon, Y. M. M. Antar, D. Roscoe and M. Cuhaci, "Recent Advances in Dielectric Resonator Antenna Technology", IEEE Transaction on Antenna and Propagation Magazine, Vol. 40, 1998, pp. 35-48.

[11] R. K. Mongia, A. Ittipiboon, P. Bharita, and M. Cuhaci, "Electric Monopole Antenna Using a Dielectric Ring Resonator", Electronics Letters, vol. 29, pp. 1530-1531, 1993.

[12] Neshati M. H. and Wu, Z., "Probe-Fed Rectangular Dielectric Resonator Antennas: Theoretical Modeling & Experiments.", 10th Iranian Conference on Electrical Engineering, May 14-16, 2002, Tabriz University, Tabriz, Iran, Communication Proceedings Vol. 2 pp. 573-579.

[13] Balanis C. A., Advanced Engineering Electromagnetic, John Wiley & Sons, 1989.

[14] Balanis C. A., Antenna Theory, Analysis and Design, John Wiley & Sons, 1997.

[15] Z. Wu, and L.E. Davis, "Automation-oriented technique for quality-factor measurement of high-T_c super-conducting resonators", IEE Proceedings Science and Measurement Technology, Vol.141, No. 6, 1994, pp 527-530.

[16] Hewlett-Packard Company, "HP85180A High-Frequency Structure Simulator (HFSS): User's Reference", 1994.